Effects of Tetramethoxystilbene on Hormone-Resistant Breast Cancer Cells: Biological and Biochemical Mechanisms of Action

Hoyong Park,[1,3] Sarah E. Aiyar,[1] Ping Fan,[1] Jiping Wang,[1] Wei Yue,[1] Tatiana Okouneva,[4] Corey Cox,[4] Mary Ann Jordan,[4] Laurence Demers,[5] Hyungjun Cho,[2] Sanghee Kim,[6] Robert X.-D. Song,[1] and Richard J. Santen[1]

[1]Endocrinology and Metabolism and [2]Biostatistics, University of Virginia Health System, Charlottesville, Virginia; [3]Department of Surgery, Kyungpook National University Hospital, Daegu, South Korea; [4]Neuroscience Research Institute, University of California, Santa Barbara, California; [5]Core Endocrine Laboratory, Pennsylvania State University College of Medicine, Hershey, Pennsylvania; and [6]Natural Products Research Institute, College of Pharmacy, Seoul National University, Seoul, South Korea

Abstract

Secondary resistance to hormonal therapy for breast cancer commonly develops after an initial response to tamoxifen or aromatase inhibitors. Agents to abrogate these adaptive changes would substantially enhance the long-term benefits of hormonal therapy. Our studies with a stilbene derivative called TMS (2,3′,4,5′-tetramethoxystilbene) identified unexpected effects with potential utility for treatment of breast tumors secondarily resistant to hormonal therapy. TMS was originally developed as an inhibitor of cytochrome P450 1B1 to block the conversion of estradiol to 4-OH-estradiol. While studying this agent in three models of hormone resistance, we detected direct antitumor effects not related to its role as an inhibitor of catecholestrogens. During examination of the mechanisms involved, we showed that treatment with 3 μmol/L TMS for 24 h inhibited tubulin polymerization and microtubule formation, caused a cell cycle block at the G_2-M phase, and induced apoptosis. TMS also inhibited activated focal adhesion kinase (FAK), Akt, and mammalian target of rapamycin (mTOR) and stimulated c-jun-NH_2-kinase and p38 mitogen-activated protein kinase activity. With respect to antitumor effects, TMS at a concentrations of 0.2 to 0.3 μmol/L inhibited the growth of long-term tamoxifen-treated MCF-7 cells by 80% and fulvestrant-treated MCF-7 cells by 70%. *In vivo* studies, involving 8 weeks of treatment with TMS via a 30-mg s.c. implant, reduced tumor volume of tamoxifen-resistant MCF-7 breast cancer xenografts by 53%. Our data suggest that TMS is a promising therapeutic agent because of its unique ability to block several pathways involved in the development of hormone resistance. [Cancer Res 2007;67(12):5717–26]

Introduction

Two-thirds of breast cancers, when excised at the time of original diagnosis in women, contain estrogen or progesterone receptors (1). The presence of these receptors predicts that hormonal therapy will induce objective disease regressions lasting for 12 to 18 months on average in the majority of patients with advanced disease. However, tumor regrowth then occurs as a reflection of the development of secondary hormonal resistance. Substantial investigative effort has focused recently on the mechanisms potentially responsible for secondary resistance (2–6). Comprehensive studies in breast cancer model systems have led to the concept that cancer cells dynamically adapt in response to various antihormonal therapies and up-regulate growth factor pathways as a mechanism for resistance (2, 6, 7).

Women who have developed secondary resistance to one hormonal therapy may often respond to a second- or third-line hormonal therapy (1). However, nearly all women ultimately become completely resistant and require alternative treatment approaches, which generally involve cytotoxic chemotherapy (1). Because of the side effects and toxicity associated with chemotherapy, therapy targeted to more specific intracellular signaling events is a major focus of current research. The crosstalk between estrogen receptors (ER) and growth factor receptor pathways in secondarily resistant ER + breast cancer cells has suggested the use of inhibitors of growth factor pathways rather than chemotherapy at this stage of the disease (8). Both preclinical and early-phase clinical trials are testing various combinations of inhibitors and particularly those targeting the EGF-R, HER-2, and mammalian target of rapamycin (mTOR) pathways. Potential drawbacks are that these agents can produce significant toxicity in the heart and other organs, and that treatment might not be focused on targets that are up-regulated in the individual patient. Based on these concepts, a relatively nontoxic agent that would act upon multiple targets but exert minimal toxicity would be a welcome addition to the therapeutic armamentarium.

During the course of our studies, we identified unexpected properties of a drug, called tetramethoxystilbene (TMS), a synthetic derivative of the herbal product, rhapontigenin (9). Rhapontigenin, a naturally occurring stilbene, is a potent mechanism-based inactivator of cytochrome P450 1A1(10). *Trans*-stilbene compounds have been chemically modified with the goal of creating anticancer agents with a higher potency of inhibition against cytochrome P450 1B1, an enzyme that catalyzes the formation of potentially genotoxic estradiol metabolites (9–12). Naturally occurring stilbenes have dihydroxyl groups on their phenyl ring. Because substitution of dihydroxyl for dimethoxy groups was thought to increase the lipophilicity and binding to the active sites of the P450 family 1 enzymes, TMS was synthesized such that dimethoxy groups were placed on the 3 and 5 positions of the phenyl ring. TMS, a methoxy derivative of 2,4,3′,5′-tetrahydroxystilbene, showed potent and selective inhibition of P450 1B1 (9–11). The original rationale of our studies was to evaluate the effect of TMS on the conversion of estradiol to 4-OH-estradiol and ultimately on tumor formation (12). However, we

Note: Supplementary data for this article are available at Cancer Research Online (http://cancerres.aacrjournals.org/).

H. Park and S.E. Aiyar are co–first authors.

Requests for reprints: Richard J. Santen, Department of Internal Medicine, University of Virginia, P.O. Box 801416, Charlottesville, VA 22908. Phone: 434-924-2207; Fax: 434-924-1284; E-mail: rjs5y@virginia.edu.

doi:10.1158/0008-5472.CAN-07-0056

observed that TMS was highly effective in reducing cell number in breast cancer cells in tissue culture. In an attempt to uncover the mechanisms responsible for this effect, we discovered "off-target" actions including a marked inhibition of microtubule polymerization, substantial induction of apoptosis, and effects on several growth factor signaling molecules.

This manuscript describes the effects of TMS on microtubule polymerization, cell cycle dynamics, growth factor pathways, and apoptosis. We found that this agent induces apoptosis in 80% to 90% of cells within a 48-h period and inhibits breast cancer cells with secondary hormonal resistance more effectively *in vivo* and *in vitro* than hormone-dependent cells. Based on its lack of apparent toxicity in intact animals, its antitumor effects *in vitro* and *in vivo*, and its potent actions on cell signaling pathways, we believe that this agent could potentially serve as an important therapeutic agent for the treatment of women who develop secondary resistance to hormonal therapy.

Materials and Methods

Reagents. TMS was synthesized as described previously (9). Tamoxifen (TAM) and fulvestrant (ICI 182,780–ICI) were purchased from Sigma. Sources of antibodies for Western analysis include Zymed Laboratories, Inc. for total and phosphospecific mitogen-activated protein kinase (MAPK) monoclonal antibodies and Cell Signaling Technology for Ser^{473}-phospho-Akt, total Akt, Thr^{389}-phospho-p70 S6K, total p70 S6K, Ser^{65}-phospho-4E-BP1, total 4E-BP1, Tyr^{1068}-phospho-EGF receptor, and $Tyr^{576/577}$-phospho–focal adhesion kinase (FAK) and Santa Cruz Biotechnology for ERα. Cell culture medium (IMEM) was from Biosource International, Inc. Fetal bovine serum (FBS), glutamine, and trypsin were from Invitrogen. z-VAD was purchased from Calbiochem and was dissolved in dimethylsulfoxide (Sigma Chemical Co.). Dextran-coated charcoal-stripped FBS (DCC-FBS) was prepared as previously described (2).

Cell culture conditions. Wild-type MCF-7 cells were grown in IMEM containing 5% FBS. Tamoxifen-resistant (TAM-R) MCF-7 cells were treated with tamoxifen (10^{-7} M) continuously for more than 1 year with a change in medium every 2 to 3 days (13). ICI 182,780 (ICI)–resistant MCF-7 cells were treated with ICI (ICI 10^{-8} M) continuously over a period of more than 1 year. Long-term estradiol-deprived (LTED) cells were developed as previously described (14) and maintained routinely in phenol red–free IMEM supplemented with 5% DCC-FBS.

Assessment of cell growth. Cells were plated in six-well plates at a density of 60,000 cells per well in their culture media. Two days later, the cells were treated as described in figure legends for 5 days with media change on day 3. Nuclei were prepared by sequential addition of 1 mL HEPES-$MgCl_2$ solution (0.01 mol/L HEPES and 1.5 mmol/L $MgCl_2$) and 0.1 mL ZAP solution [0.13 mol/L ethylhexadecyldimethylammonium bromide in 3% glacial acetic acid(v/v)] and counted using a model Z1 Coulter counter (Coulter Corp).

Cell proliferation. To specifically assess cell proliferation, ^{3}H-thymidine incorporation into DNA was assessed by methods previously described (15).

Plasma estradiol assay. Estradiol was measured with a previously described RIA method involving purification with column chromatography and use of an iodinated estradiol trace (Diagnostic Products Corp.). Assay sensitivity is 5 pg/mL, and interassay precision averages 11% at a concentration of 32 pg/mL (16).

Immunoblotting. Cells were grown to 80% confluence in 60-mm dishes and lysed with buffer containing 20 mmol/L Tris (pH, 7.5), 150 mmol/L NaCl, 1 mmol/L EDTA, 1 mmol/L EGTA, 1 mmol/L sodium orthovanadate, 2.5 mmol/L sodium PPi, 1% Triton X-100, 1 mmol/L β-glycerophosphate, 1 μg/mL leupeptin and aprotinin, 1 mmol/L phenylmethylsulfonyl fluoride. Cells were then pulse sonicated for 30 s at room temperature and centrifuged at 14,000 rpm for 10 min. Cell lysates were stored at −80°C. The total protein concentration was determined using a standard Bradford assay reagent (Bio-Rad). Western blots were carried out using primary antibodies dissolved in PBS containing 5% bovine serum albumin (BSA); secondary antibody conjugated with horseradish peroxidase (1:2,000); and SuperSignal West Pico Chemiluminescent Substrate (Pierce) to identify bands on X-ray film.

Apoptotic cell death detection by ELISA. To quantitate histone-associated DNA fragments (mono- and oligonucleosomes) *in vitro* in the cytoplasm of MCF-7 cells undergoing early apoptosis, ~8×10^4 MCF-7 cells were plated per well into 12-well plates. After 2 days, the cells were treated with either DMSO, 3 μmol/L TMS, or 10 nmol/L 17β-estradiol + 3 μmol/L TMS. After 24 h, floating cells and adherent cells were collected for analysis. A cell death detection $ELISA^{PLUS}$ apoptosis kit (Roche) was used as described by the manufacturer. Experiments were done in triplicate, and *P* values were determined using SigmaPlot (Systat Software Inc.).

Measurement of DNA degradation via terminal nucleotidyl transferase–mediated nick end labeling assay. Apoptotic MCF-7 cells were detected by terminal nucleotidyl transferase–mediated nick end labeling (TUNEL) using the APO-BRDU Complete Flow Cytometry Analysis Kit (Phoenix Flow Systems, Inc.) according to the manufacturer's protocol. Controls included positive and negative cells provided in the kit following the manufacturer's protocol.

Cell cycle distribution. MCF-7 cells were grown in IMEM + 5% FBS. Cells were treated with either DMSO or TMS for 12, 24, 36, or 48 h. Both floating and adherent cells were collected and filtered through a 40-μm cell strainer (BD Falcon) to remove clumps. Cells were counted, and 1×10^6 cells were hypotonically lysed in 1 mL of DNA staining solution [3.4 mmol/L Tris (pH, 7.6), 0.075 mmol/L propidium iodide (PI), 0.1% NP40, and 700 units/L RNase A] for 10 min on ice. Samples were then analyzed on a FACSCalibur flow cytometer (Becton Dickinson), and cell cycle distribution and percentage of cells within the sub-G_1 peak were determined using Modfit software (DNA Modelling System, Verity Software House, Inc.).

Annexin V assay. MCF-7 cells were treated with either DMSO or 3 μmol/L TMS for 12, 24, 36, or 48 h. Floating cells were collected by centrifugation and added to adherent cells, which were gently lifted off the tissue culture plate with Accutase (Innovative Cell Technologies, Inc.). A total of 20,000 MCF-7 cells were labeled with Annexin V–Alexa 488 antibody and PI using an apoptosis detection kit (Invitrogen) and analyzed on a FACScalibur flow cytometer (Becton Dickinson). The distribution of apoptosis was determined using Cell QuestCell software (Becton Dickinson), and cells that were Annexin V (−) and PI (−) were considered viable cells. Cells that were Annexin V (+) and PI (−) were considered early-stage apoptotic cells. Cells that were Annexin V (+) and PI (+) were considered late-stage apoptotic cells. Cells that were PI (+) and Annexin V (−) were considered necrotic.

Immunofluorescence microscopy. MCF-7 cells were grown for 24 h on coverslips pretreated with poly-lysine to enhance cell flattening and adherence and then incubated in the presence or absence of TMS (0.1, 1, 5, 10, and 50 μmol/L) for 20 h. Control cells were incubated with vehicle alone. Cells were fixed in 10% formalin (20 min, 25°C) and permeabilized in methanol (−20°, 10 min). Nonspecific antibody staining was blocked with 20% normal goat serum in PBS, and cells were incubated with DM1a anti–α-tubulin antibody (Sigma Chemicals; 1:1,000 dilution) followed by goat anti-mouse FITC-conjugated secondary antibody (Sigma Chemicals; 1:500 dilution) for 1 h at 37°C to visualize microtubules. Nuclei were stained with 4′,6-diamidino-2-phenylindole (0.2 μg/mL in PBS; Sigma Chemicals) for 1 min. Coverslips were mounted with Prolong Antifade (Molecular Probes) and viewed and photographed with a 60× objective using an ORCA II digital camera driven by Metamorph software (Universal Imaging) on a Nikon Eclipse E800 fluorescence microscope.

Purification of tubulin and microtubule polymerization. Microtubule protein preparations consisting of tubulin and microtubule-associated proteins were isolated from bovine brain by three cycles of polymerization and depolymerization. Tubulin was purified from the microtubule protein by phosphocellulose chromatography, drop-frozen in liquid nitrogen, and stored at −70°C (17). On the day of use, tubulin was thawed on ice and centrifuged (17,000 × *g*, 20 min, 4°C) to remove aggregated or denatured tubulin. Protein concentration was determined by Bradford assay using BSA as standard. For polymerization, tubulin (2.75 mg/mL) was mixed

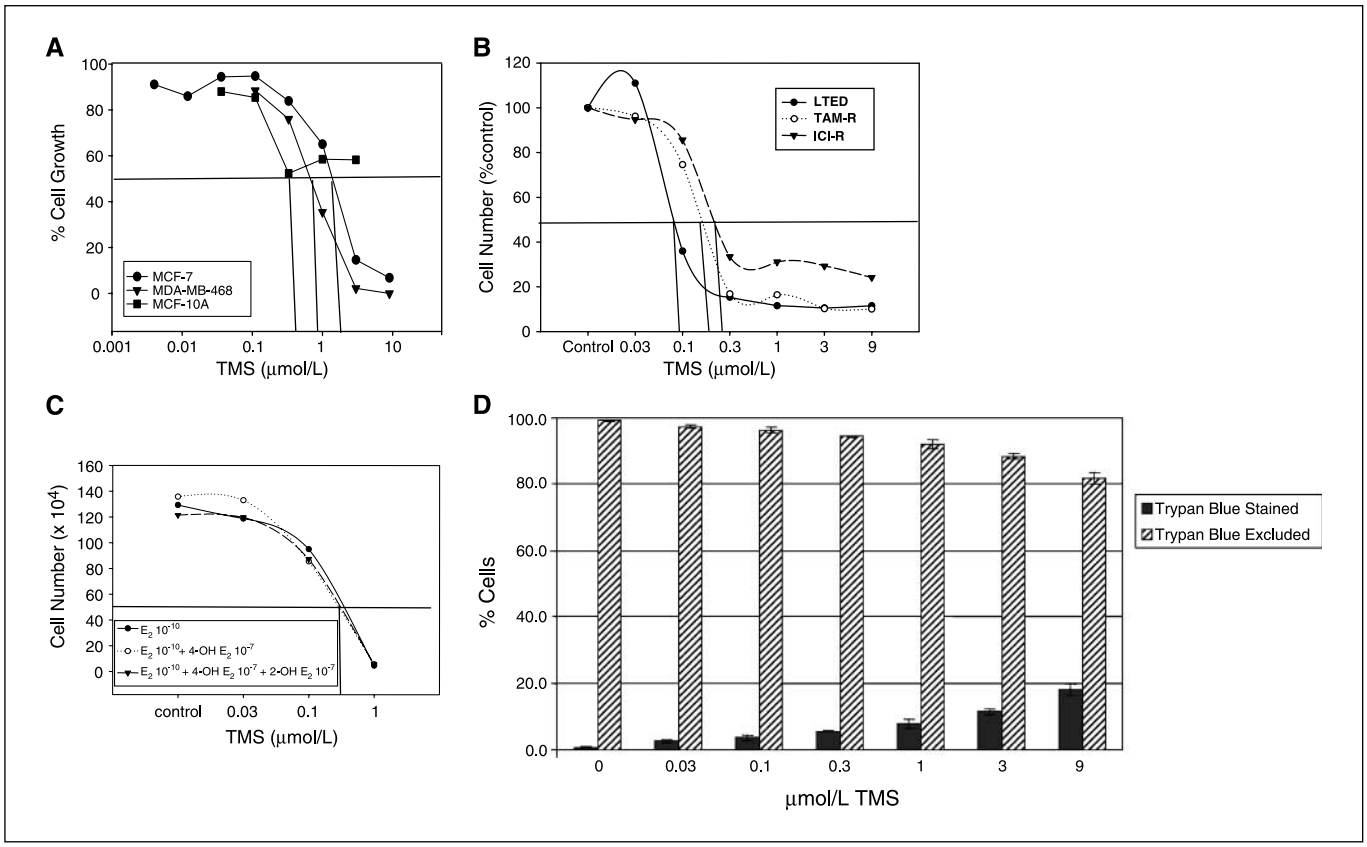

Figure 1. TMS inhibits hormone-resistant MCF-7 cell number. *A,* hormone-dependent parental MCF-7 cancer cells, hormone-independent MDA-MB-468 cells, and benign MCF-10A cells were treated with TMS for 5 d with cell counts at that time point. To normalize results among experiments, results are expressed as percent of vehicle control cell number. *B,* LTED (long-term estradiol deprived MCF-7 cells), TAM-R (long-term tamoxifen-treated MCF-7 cells), ICI-R (ICI-resistant MCF-7 cells) under similar conditions. *C,* estradiol (10^{-10}), 4-OH-estradiol (10^{-7}) and 2-OH-estradiol (10^{-7}) metabolites were added to the medium with TMS. *D,* trypan blue exclusion test indicates that TMS-treated cells are largely viable at the 24-h time period.

with a range of concentrations of TMS in 100 mmol/L PIPES, 1 mmol/L $MgCl_2$, 1 mmol/L EGTA, and 1 mmol/L GTP. Microtubule seeds were prepared with the same solution (without TMS) plus 10% glycerol and 10% DMSO by incubating at 30°C for 30 min and shearing the assembled microtubules six times through a 25G 7/8 in needle. Microtubule polymerization was initiated by adding seeds to the tubulin solution and was monitored at 30°C by light scattering at 350 nm using a Beckman DU 640 spectrophotometer.

Mouse xenograft model. Tumor fragments (30–40 mg) of TAM-R MCF-7 human mammary tumors were implanted s.c. as xenografts in oophorectomized nude mice (Charles River Labs) aged 4 to 5 weeks at the start of the experiment. Animals containing continuously passaged tumors in tamoxifen-treated animals were obtained as a gift from V.C. Jordan (Fox Chase Cancer Center, Philadelphia, PA; ref. 18). Estradiol was delivered to produce plasma levels of 280 pg/mL with an "estradiol clamp," silastic capsule method previously described (19). Treatment with s.c. silastic capsules containing 30 mg TMS was started when tumors reached a measurable size ($\sim$300 mm^3), about 6 months after inoculation. Tumors were measured at least weekly with calipers, and volumes were calculated using the formula $4/3\pi \times r_1^2 \times r_2$ ($r_1 < r_2$) during 8 weeks. All animal experiments were conducted under Federal and Institutional guidelines and approved by the University of Virginia Animal Care and Use Committee.

Statistical analysis. Statistical analysis was done by using the *R* statistical package.[7] A mixed-effect linear model with two fixed effects (day and drug) and a random effect (mouse) was fitted, and the statistical significance of the drug effect was examined with the significance level 0.05. In particular, $\log_{10}$ transformation was used for MCF tumor volume data to produce a linear relationship between tumor volumes and days.

Results

The effects of TMS on breast cancer cell growth. Initially, we tested the effect of TMS on growth of several breast cell lines, including benign ER-negative MCF10A, malignant receptor–negative MDA-MB-468, and hormone-dependent parental MCF-7 cells and three varieties of secondarily hormone-resistant MCF-7 cell lines (TAM-R, fulvestrant-resistant and LTED).

TMS inhibited the wild-type MCF-7 and MDA-MB-468 cells by 50% at a concentration of $\sim$1 μmol/L with greater suppression at higher doses (Fig. 1*A*). The benign MCF10A cells were inhibited by 50% at a similar concentration, but with a plateau at higher doses. All three secondarily resistant cells lines were inhibited by 50% at TMS concentrations of $\sim$0.1 to 0.3 μmol/L (Fig. 1*B*). With increasing doses, the cells exhibited a 70% to 90% reduction in cell number in a dose response fashion with increasing concentration of TMS until a plateau was reached at 0.3 to 1 μmol/L (see Fig. 1*B*).

TMS is known to inhibit the cytochrome P450 1A1 and 1B1 enzymes and, thus, to reduce the conversion of estradiol to

[7] http://www.r-project.org/

2-hydroxyestradiol and 4-hydroxyestradiol. Other investigators have shown that these catecholestrogens could potentially stimulate proliferation of breast cancer cells (20). Accordingly, we considered that TMS might inhibit cell number by blocking 4-hydroxylation of estradiol. To examine this possibility, we attempted to rescue the cells from TMS blockade by adding the products of these enzymes, 2-OH- and 4-OH-estradiol, respectively, as well as the substrate estradiol, to the cells receiving TMS. All three cell lines exhibited a similar degree of inhibition of cell number in the presence of added 2-OH-estradiol and of 4-OH-estradiol, as well as estradiol itself. These results clearly indicated that the mechanism of TMS to reduce cell number was not mediated by the inhibitory effects of TMS on cytochrome P450 1A1 and 1B1 with the resulting reduction of catecholestrogen formation (see Fig. 1*C*).

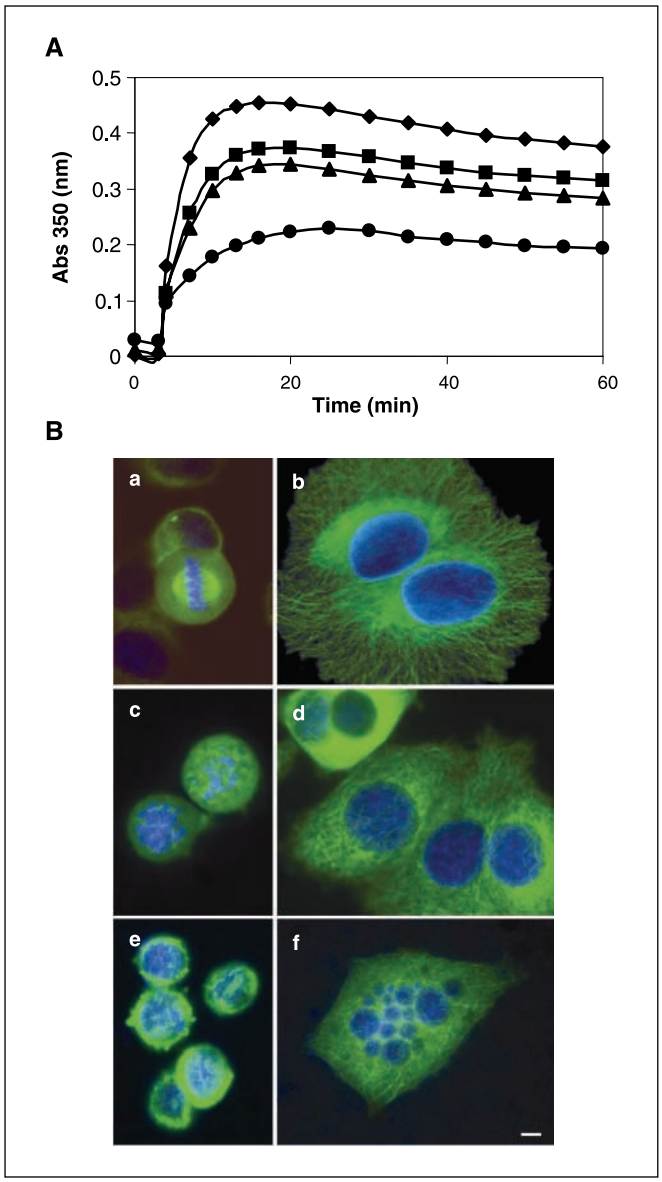

Figure 2. *A,* TMS effects on tubulin polymer mass and mitosis. Purified tubulin was assembled to steady state in the absence or presence of a range of concentrations of TMS (0.3–3 μmol/L) by adding 1 part microtubule seeds to 50 parts tubulin at 30°C and monitoring turbidity spectophotometrically for 60 min. Control (♦), 0.3 μmol/L (■), 1 μmol/L (▲), 3 μmol/L (●). Microtubule polymerization was inhibited in a TMS concentration–dependent manner. TMS (3 μmol/L) inhibited polymer mass by 50%. *B,* effects of TMS on microtubule organization in cells. Immunofluorescence images of microtubules (*green*) and DNA (*blue*) in fixed cells in the presence or absence of TMS. *a* and *b,* untreated control cells. The remaining photos illustrate TMS-treated cells: *c,* 1 μmol/L TMS; *d,* 10 μmol/L TMS; *e,* 50 μmol/L TMS; *f,* 10 μmol/L TMS. In control mitotic cells (*a*), spindles were bipolar, and all chromosomes were congressed to a compact metaphase plate. However, in the presence of 1 μmol/L TMS (*c*), mitotic cells contained multiple asters of very short microtubules and chromosomes were disorganized. Interphase control cells (*b*) and interphase cells incubated with 1 μmol/L (*d*) or 10 μmol/L TMS (*e*) exhibited microtubules, but the cells were less well spread in the presence of TMS, and the overall microtubule polymer was reduced. Microtubules were depolymerized, and the cytoplasm was severely reduced after incubation with 50 μmol/L TMS (*e*). TMS incubation induced frequent multinucleated cells (*d, top cell*, and *f*). *Bar,* 5 μm.

We then questioned whether the TMS effects might represent generalized toxicity to the breast cancer cells with resulting increase in necrotic cell death, as evidenced by trypan blue uptake at 24 h of exposure to TMS. Surprisingly, a large fraction of the secondarily resistant cells detached from the culture plates (see Supplementary Fig. S1) in response to TMS. The parental MCF-7 cells seemed less sensitive to this effect of TMS, as shown above for inhibition of cell growth (Fig. 1*A*). Although detached, these cells were still able to exclude trypan blue, a finding that excluded necrotic cell death and provided evidence of continued viability (Fig. 1*D*).

Effects of TMS on tubulin polymer mass and mitosis. The detachment of viable cells at 24 h suggested that TMS might exert specific effects on cellular structures that mediate adherence to culture plate surfaces. Resveratrol, a stilbene with a structure similar to TMS, had been reported to interfere with microtubule function (21). Accordingly, we examined the effect of TMS on microtubule polymerization. A microtubule polymerization assay was used to study this phenomenon. Concentrations of TMS ranging from 0.3 to 3.0 μmol/L inhibited microtubule polymerization in a time and dose response fashion, with a maximum inhibition of 50% of vehicle control (Fig. 2*A*).

The effects of TMS on microtubule organization in cells. The effects of TMS (1–50 μmol/L) on microtubule arrays and chromatin in fixed MCF-7 cells are shown in Fig. 2*B*. TMS induced highly abnormal mitotic spindles and multinucleated cells. In control mitotic cells, most spindles were bipolar (Fig. 2*Ba*), with all the chromosomes congressed to a compact metaphase plate and interphase cells (Fig. 2*Bb*) were well spread with an array of fine filamentous microtubules. At 1 μmol/L TMS (Fig. 2*Bc*), mitotic microtubules were very short and stubby and arranged in multiple asters, and chromosomes were in a disorganized ball-shaped mass. Interphase cells at 1 and 10 μmol/L TMS (Fig. 2*Bd* and *f*) contained intact microtubules, but the overall mass of microtubules was reduced, and the cells were less well spread. At 50 μmol/L TMS (Fig. 2*Be*), cells were small and had very little cytoplasm, and microtubules seemed depolymerized. In addition, after incubation with TMS (1–50 μmol/L), many cells became multinucleated (Fig. 2*Bd* and *f*), a phenomenon that is often seen after escape from mitotic arrest induced by microtubule-targeted drugs (22).

TMS induces G_2-M cell cycle arrest. Blockade of microtubule polymerization can result in arrest of the cell cycle at the S or G_2-M phase depending on the specific microtubule polymerization agent used (23). We carried out fluorescence-activated cell sorting analysis using PI to stain DNA and examined MCF-7 cells that had been treated for 12, 24, 36, and 48 h in the absence or presence of 3 μmol/L TMS. We found that at 36 h, a large percentage of the TMS-treated cells were arrested in the G_2-M phase of the cell cycle

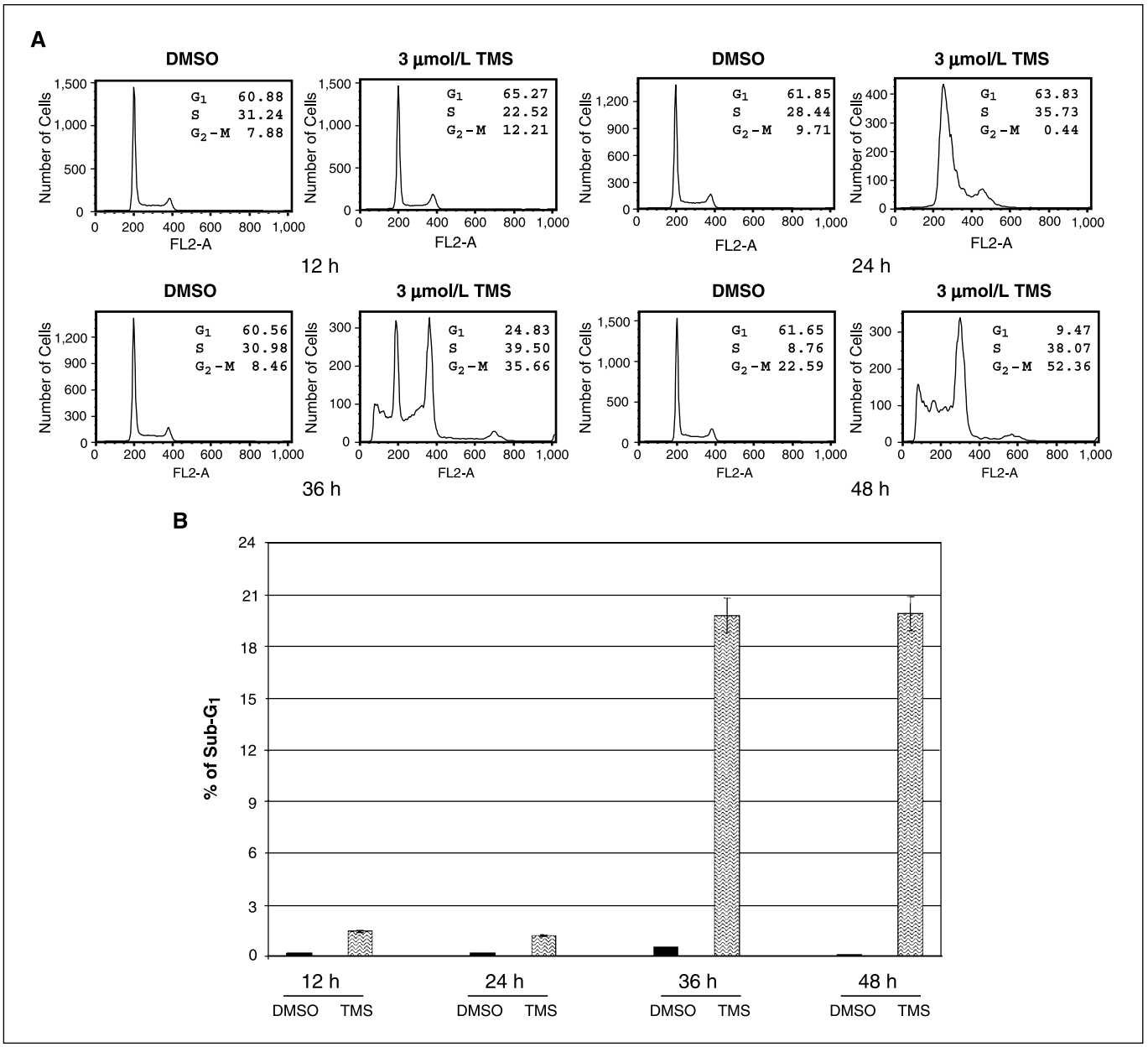

Figure 3. TMS induces G_2-M cell cycle arrest in MCF-7 breast cancer cells. *A,* cell cycle analysis of MCF-7 cells after treatment with 0.1% DMSO or 3 μmol/L TMS. After 12, 24, 36, and 48 h of treatment, cells were labeled with PI and analyzed by DNA flow cytometry. The fraction of cells in the G_1, S, and G_2-M phases at the indicated times are shown by the numbers included in the panels. The percent of cells in the sub-G_1 phase is shown in (*A*) and quantitated in (*B*).

when compared with the control DMSO-treated cells (Fig. 3*A*, compare G_1 with G_2-M peaks). The increased G_2-M peak is consistent with what has been reported for the microtubule inhibitor nocodazole (24). In addition, after 48 h treatment with 3 μmol/L TMS, we observed a sub-G_1 peak that is apparent in Fig. 3*A* (*bottom right*), suggesting the possibility of apoptosis. Modfit was used to quantitate the sub-G_1 peak, and an increase from 2% at 12 h to a maximum of 20% at 36 and 48 h (Fig. 3*B*) was observed. The sub-G_1 peak was negligible in the DMSO-treated control cells.

The flow cytometry studies indicated a cell cycle arrest, but were not optimized to detect an inhibition of DNA synthesis. For that reason, we conducted ^{3}H-thymidine uptake experiments to directly examine the effect of TMS on DNA synthesis. Under conditions of high and low serum concentrations, 3 μmol/L TMS caused a 50% inhibition of ^{3}H-thymidine uptake (Supplementary Fig. S2).

TMS induces apoptosis in breast cancer cells. The presence of viable (i.e., trypan blue excluding) floating cells at 24 h and the sub-G_1 peak on flow cytometry suggested that TMS triggers apoptosis. To distinguish apoptosis from necrosis at later time points, we examined Annexin V and PI staining followed by flow cytometry. We found that at 12 h, only 6% of the TMS-treated cells were apoptotic (see Supplementary Fig. S3, compare DMSO-treated to TMS, sum of early and late apoptosis). At 24 h, apoptosis increased to 12%, and at 36 and 48 h, apoptosis increased to 40%.

During each time point, the maximum percent of necrotic cells in the TMS-treated groups was 0.73% compared with 0.88% in the DMSO-treated cells (Supplementary Fig. S3, compare top left quadrant DMSO to TMS).

As further evidence of apoptosis, we carried out an anti-histone/DNA monoclonal antibody ELISA assay, which examines double-strand DNA breaks occurring at an early stage. Three cell lines, parental, LTED, and Tam-R, were treated with either ethanol, 3 μmol/L TMS, or 3 μmol/L TMS + 10 nmol/L E2 for 24 h and assayed by ELISA. We found that addition of 3 μmol/L TMS resulted in an increase in the level of dsDNA and nucleosomes present in the cytoplasm (Fig. 4*A–C* compare *lanes 1* to *2*). Because it is known that the microtubule active agent, paclitaxel, is inhibited in the presence of estradiol, we also tested whether the addition of estradiol would inhibit the action of TMS in these cell lines (25, 26). When 10 nmol/L E2 was added in the presence of TMS, there was no decrease in the level of apoptosis for the parental or LTED cells (Fig. 4*A* and *B*, compare *lanes 2* with *3*) and only a slight decrease in the TAM-R cells (Fig. 4*C*, compare *lanes 2* with *3*). Most, but not all, types of programmed cell death involve activation of caspases (27). For this reason, we examined the effects of the pan-caspase inhibitor, z-VAD, and showed blockade of TMS-elicited apoptosis, a finding providing strong evidence for the presence of caspase-induced apoptosis (Fig. 4*A–C*, compare *lanes 2* to *4*).

We then used the TUNEL assay to detect single- and double-stranded DNA breaks as free 3′OH-termini incorporating bromodeoxyuridine (BrdUrd). Parental MCF-7 cells were treated with either DMSO or 3 μmol/L TMS for 24 h (*top*), 36 h (*middle*) or 48 h (*bottom*; Fig. 4*D*). No significant level of BrdUrd was incorporated into the control or TMS-treated cells at 24 h (Fig. 4*D* compare *left top* to *right top*). At 36 and 48 h, 83% of the TMS-treated cells contained apoptotic nuclei as compared with only 1.6% in the control cells exposed to DMSO.

Most types of apoptosis involve the cleavage of poly(ADP-ribose) polymerase (PARP) as molecular signature of apoptosis (28). We therefore examined the effect of TMS on the cleavage of this protein and the ability of the pan-caspase inhibitor z-VAD to block these effects. TMS caused an increase in the p85

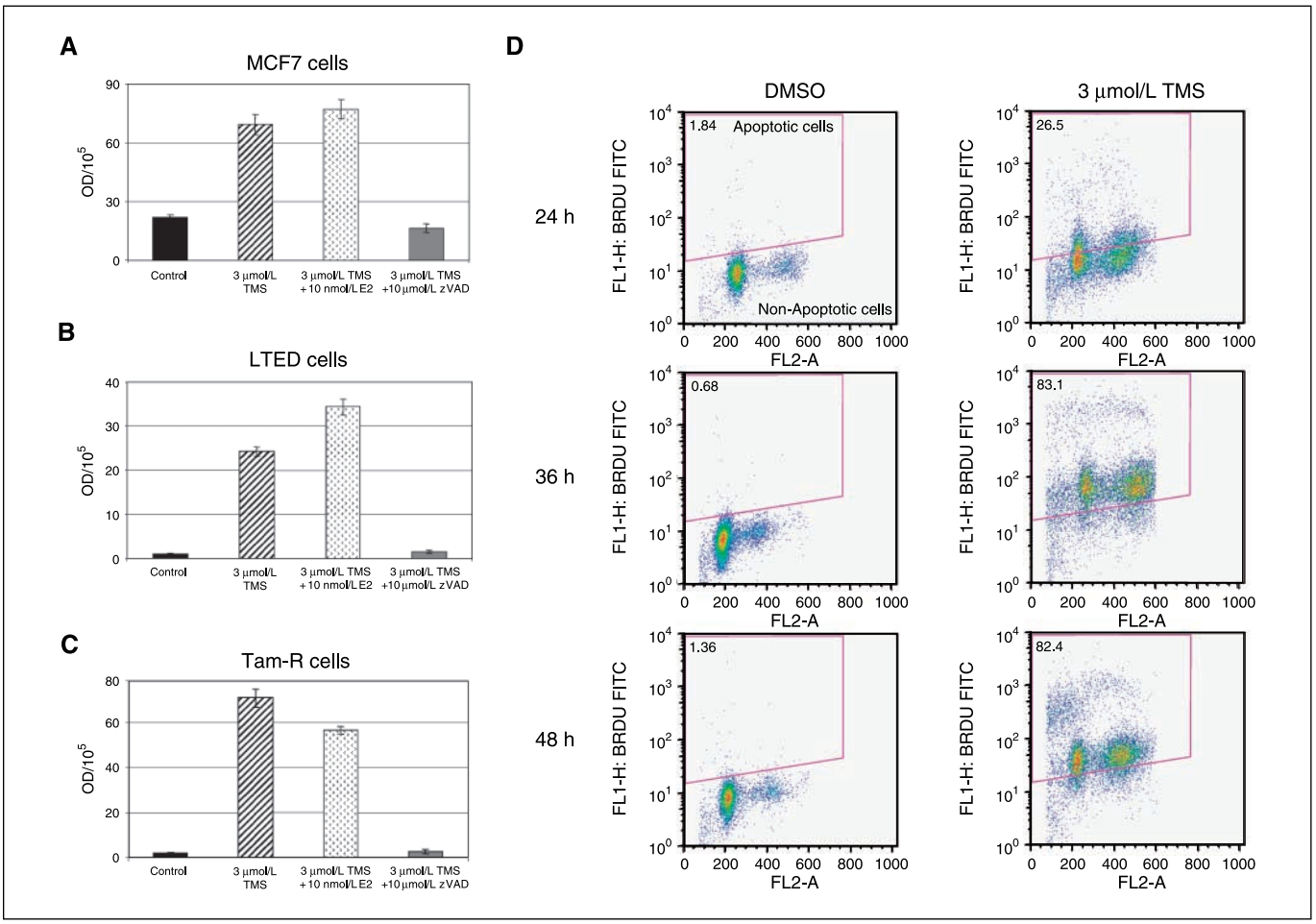

Figure 4. TMS induces cell death. *A,* MCF-7 cells were treated with TMS (3 μmol/L) for 24 h. ELISA cell death detection kit showed that TMS increases apoptosis three times higher than control. Estradiol did not block TMS effects. *B,* LTED cells show more apoptosis with the E2 plus TMS treatment than with the TMS treatment alone based on OD/10^5 at 24 h. *C,* estradiol blocked TMS effects slightly in TAM-R cells. *D,* MCF-7 cells were harvested and studied with APO-BRDU TUNEL assay. MCF-7 cells were treated with 0.1% DMSO or 3 μmol/L TMS for 24, 36, or 48 h. Cells were double-stained with BrdUrd and PI and analyzed for apoptosis by DNA flow cytometry. The numbers in the boxes indicate the percentage of BrdUrd-positive cells. DMSO showed 1.36% apoptosis among live cell population, but 3 μmol/L TMS treatment for 48 h induced 82.4% apoptosis.

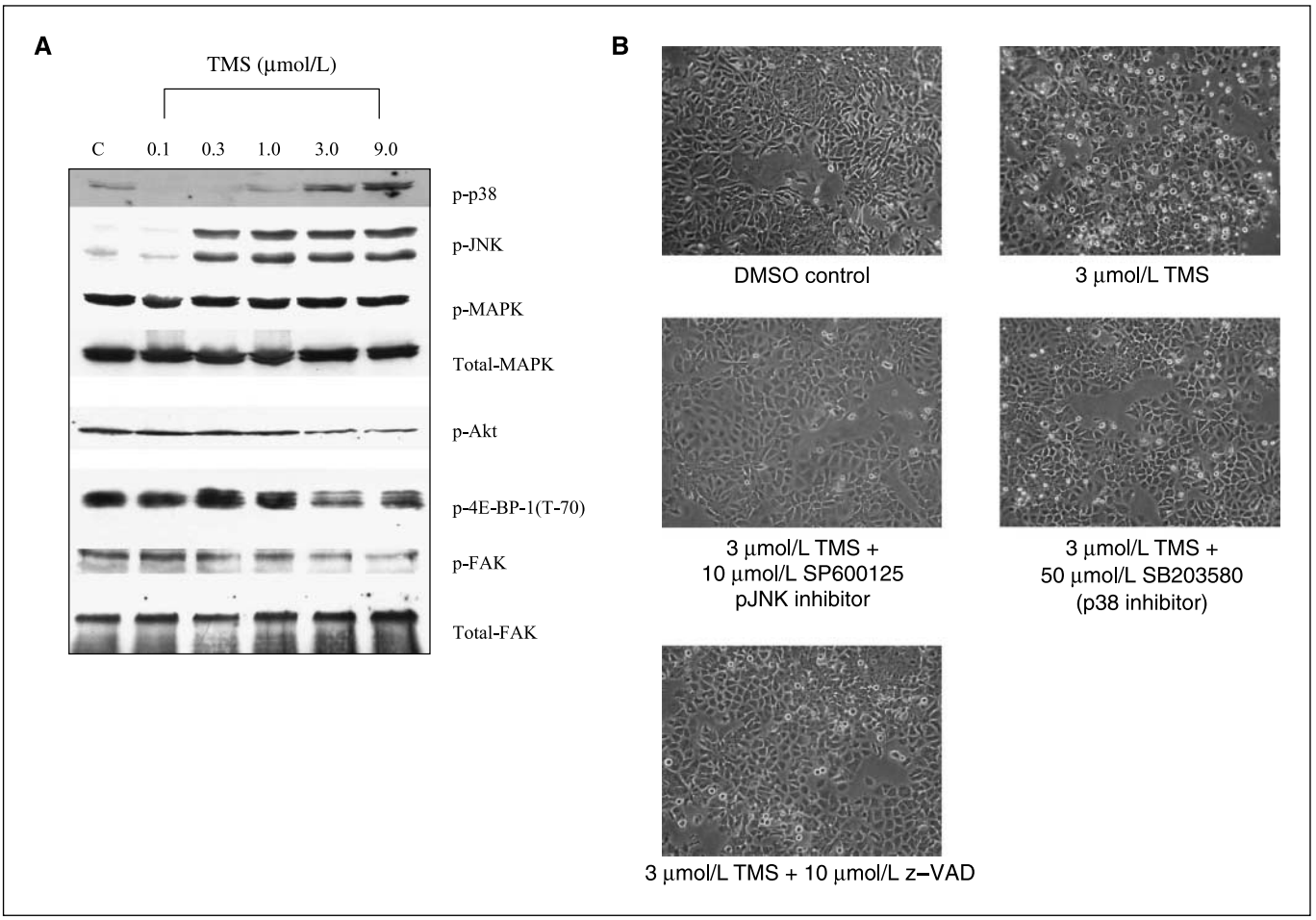

Figure 5. TMS can inhibit multiple signal pathways. *A,* lysates were prepared at different concentrations of TMS with MCF-7 cells with 24 h treatment. Protein expression levels were analyzed by Western blotting using phosphospecific antibodies against MAPK, p38, JNK, Akt, 4-E-BP-1 and FAK. *B*, Parental MCF-7 cells after 24 h treatment with TMS with JNK and p38 inhibitors and assessment of their effects on floating cells.

cleavage product of PARP, an effect blocked by z-VAD (see Supplementary Fig. S4). As an indication of the mechanism of apoptosis, the c-jun-NH_2-kinase (JNK) inhibitor (SP600125) also blocked PARP cleavage, but the p38 inhibitor (SB 203580) did not.

TMS inhibits multiple signaling pathways. Disruption of microtubules is known to trigger a sequence of downstream signaling events resulting in apoptosis (29). Accordingly, we next sought to identify the signal transduction pathways involved in regulating cell survival and cell death using Western blot techniques. Activated JNK and p-38 increased substantially with initial increases at concentrations of TMS of 0.3 and 3 μmol/L, respectively. As evidence of specificity of its effects, phospho-MAPK and total MAPK levels did not change with TMS. However, we did detect reduced phosphorylation of Akt, FAK, and 4-E-BP-1(T-70) at concentrations above 1 μmol/L (Fig. 5*A*).

Biological effects of JNK and p-38 activation. The morphologic appearance of floating cells (Fig. 5*B*) occurred during the same time frame as the activation of JNK and p38. We reasoned then that the floating cells might be used as a bioassay for JNK and p38 effects. Accordingly, we used JNK and p38 inhibitors and assessed their effects on floating cells. As shown in Fig. 5*B*, the specific inhibitors markedly decreased the number of floating cells, providing evidence that the activation of JNK and p-38 markedly influences cell detachment. As additional evidence, these inhibitors also blocked apoptosis as quantitated by the ELISA assay (Supplementary Fig. S5).

Effects of TMS on a breast xenograft model. We implanted tumor fragments (30–40 mg) of TAM-R MCF-7 human mammary tumor cells into both flanks of athymic mice. Six months after implantation of tumors, the xenografts reached measurable size ($\sim$300 mm^3). The group (n = 5) treated with vehicle alone grew substantially over the 56-day period of observation. Two months of continuous treatment with TMS, using 30 mg s.c. implants (n = 4, reduced tumor volume by 53% when compared with control (P < 0.02). In the parental MCF-7 cells xenograft model, the 30-mg TMS implant (n = 16) reduced tumor volume by 41.7% when compared with control (n = 17; Fig. 6*A*), but this effect did not reach statistical significance. Animals receiving the 30-mg implant of TMS for 2 months tolerated this procedure well and exhibited no apparent systemic toxicity. As evidence of this, there were no changes in total body weight, uterine weight (Fig. 6*B*) ovarian weight, and plasma estradiol levels and no changes in liver and renal histology (see Supplementary Figs. S6 and S7).

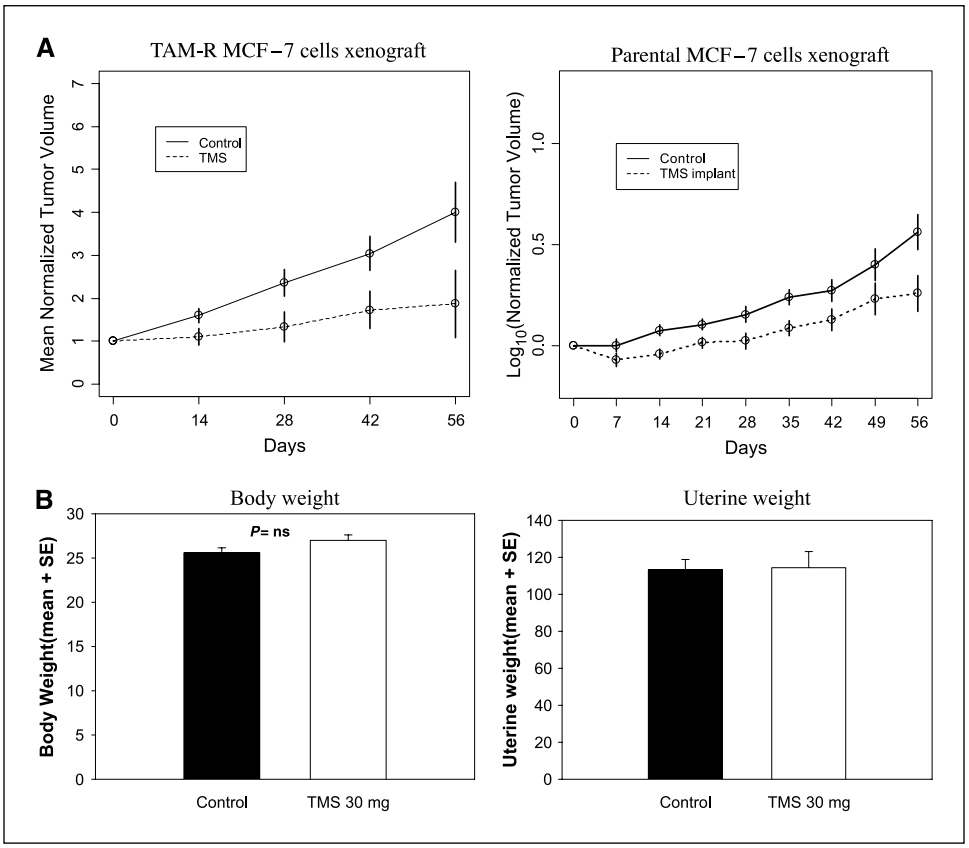

Figure 6. *In vivo* activity of TMS against MCF-7 cells xenograft model. *A,* tumor fragments (30–40 mg) of TAM-R MCF-7 human mammary tumor cells were implanted into both flanks of athymic, oophorectomized nude mice. Treatment with vehicle (n = 5) or TMS 30 mg (n = 4) s.c. implant started when tumors reached a measurable size (~300 mm^3) 6 mo after inoculation. Tumors were measured biweekly or weekly with calipers. Two months of treatment with TMS reduced tumor volume by 53% compared with control ($P < 0.02$). Parental MCF-7 cells xenograft model. TMS 30 mg implant (n = 16) reduced tumor volume by 41.7% compared with control (n = 17; $P = 0.0267$). *B,* the change in body weight and uterine weight with TMS in the MCF-7 xenograft model.

Discussion

TMS, a tetramethoxystilbene, effectively inhibits the growth of breast cancer cells engineered to become secondarily resistant to tamoxifen, fulvestrant, or estradiol deprivation, a therapeutic maneuver analogous to either use of aromatase inhibitors or surgical oophorectomy (9, 10). Although TMS was developed as an inhibitor of cytochrome P450 1B1, we showed that it exerts its effects on breast cancer cells through multiple actions, including inhibition of microtubule polymerization; blockade of cells at the G_2-M phase of the cell cycle; increase in the activation of p-38 kinase and JNK; reduction in the phosphorylation of FAK, Akt, and 4E-BP-1; and the induction of apoptosis. Notably, our studies showed that TMS inhibits the growth of TAM-R breast cancer xenografts *in vivo* without evidence of systemic or organ-specific toxicity. These properties suggest that TMS has potential as a new therapeutic approach for breast cancers that develop secondary hormonal resistance.

The effect of TMS on apoptosis *in vitro* was especially dramatic with 80–90% of cells undergoing programmed cell death by 48 h of exposure. The magnitude of this process required verification that cell death did not merely represent necrosis, and that apoptosis was indeed present. Accordingly, our study used multiple methods to provide definitive evidence of programmed cell death and the lack of necrotic toxicity. These included the use of an ELISA apoptosis assay, flow cytometry coupled with the BrdUrd-based TUNEL and Annexin V methods, demonstration of a sub-G_1 peak on flow cytometry, blockade of apoptosis with the pan-caspase inhibitor z-VAD, examination of the formation of the 89-kDa PARP cleavage product and its blockade with z-VAD, and exclusion of necrotic cell death with a trypan blue viability test. To further rule out necrotic cell death, we used the Annexin V flow cytometry–based assay and showed that a maximum of only 0.73% of cells were necrotic under all conditions examined. Taken together, these various methods provided compelling evidence of the presence of apoptosis and absence of significant necrotic cell death.

One mechanism whereby TMS induces apoptosis seems to be related to its effects on microtubule polymerization. Agents such as colchicines and nocodazole block microtubule polymerization in a manner similar to TMS and also trigger apoptosis (30). Exactly how apoptosis occurs is not completely understood, but a marked up-regulation of p-38 kinase and JNK occurs in association with this phenomenon. A suggested mechanism is that microtubule inhibitors release MLK-2 from binding to specific sites on tubulin and free it to act as an upstream kinase (MAP KKK) in the JNK kinase cascade sequence (31). JNK itself is known to mediate apoptosis under certain circumstances. Our data showing blockade of PARP cleavage with a JNK inhibitor support a role for JNK in the apoptotic process. These observations, taken in concert, would suggest that blockade of microtubule polymerization might be a primary effect of TMS and result in the secondary activation of JNK and p38 kinase. However, additional primary effects of TMS on other targets such as FAK, Akt, and mTOR might also be possible (32, 33). Further experiments are necessary to precisely determine which effects of TMS are primary and which are secondary to more upstream events.

Treatment of neoplastic diseases with other microtubule-interacting agents such as the taxanes and *Vinca* alkaloids provide effective therapy but are associated with substantial toxicity (30, 34). Our data with TMS revealed no apparent systemic toxicity at concentrations which effectively blocked growth of secondarily resistant breast cancer xenografts *in vivo*. Parameters used to assess systemic toxicity included total body weight, plasma estradiol levels, uterine and ovarian weight, and histologic changes in the liver or kidney (Supplementary Fig. S7). More detailed studies will be required to assess toxicity in greater depth and particularly neurotoxicity.

An important consideration is the relative efficacy and toxicity of TMS compared with another class of microtubule active agents, the taxanes, because both compounds exert similar actions. TMS inhibits phosphorylation of FAK, Akt, and mTOR and stimulates JNK and p38 MAPK activity. Paclitaxel also inhibits Akt and increases JNK and p38 MAPK activity (35, 36). However, paclitaxel acts differently than TMS in that it blocks microtubule depolymerization and causes stabilization of these structures. Comparative studies on antitumor efficacy, toxicity, and organ specificity will be required to fully address potential differences between these agents. An important consideration, however, is the observation that the herbal parent of TMS, rhapontigenin, has been used in oriental medicine for more than three millennia without untoward toxicity. While speculative, this would suggest that TMS, a derivative of rhapontigenin, might be relatively nontoxic as well.

Our current studies are intriguing but still contain weaknesses that we plan to address in the near future. For example, we have not as yet conducted rigorous experiments to determine if wild-type breast cancer cells of several derivations (i.e., ZR-75-1, T 47D, cloned MCF-7, or others) also seem to be less sensitive to TMS than their secondarily resistant counterparts. This could be important for concluding that TMS might be an ideal agent for treating hormone-resistant disease. However, because hormone therapy is effective initially in receptor-positive breast cancer, it is unlikely that TMS would be chosen to replace this modality of therapy. Thus, it is not essential to our conclusions that hormone-resistant cells be more sensitive to TMS than parental cells. Another issue we considered is that we did not examine DNA laddering, which is usually required for demonstration of apoptosis when using a new antiapoptotic agent. However, this technique requires the activation of caspase 3, a factor lacking in MCF-7 cells (37). Finally, it will be important in future studies to carefully examine whether TMS induces apoptosis via mitochondrial or death receptor pathways and to dissect out the precise mechanisms by which apoptosis occurs.

Acknowledgments

Received 1/15/2007; revised 2/28/2007; accepted 4/18/2007.

Grant support: NIH grant CA57291 (M.A. Jordan), and Department of Defense Breast Cancer Research Program Awards DAMD 17-03-0229 (R.J. Santen) and W81XWH-04-1-0519 (S.E. Aiyar).

The costs of publication of this article were defrayed in part by the payment of page charges. This article must therefore be hereby marked *advertisement* in accordance with 18 U.S.C. Section 1734 solely to indicate this fact.

References

1. Santen RJ, Manni A, Harvey H, Redmond C. Endocrine treatment of breast cancer in women. Endocr Rev 1990; 11:221–65.
2. Santen RJ, Song RX, Zhang Z, et al. Long-term estradiol deprivation in breast cancer cells up-regulates growth factor signaling and enhances estrogen sensitivity. Endocr Relat Cancer 2005;12 Suppl 1:61–73.
3. Gee JM, Howell A, Gullick WJ, et al. Consensus statement. Workshop on therapeutic resistance in breast cancer: impact of growth factor signalling pathways and implications for future treatment. Endocr Relat Cancer 2005;12 Suppl 1:1–7.
4. Berstein LM, Wang JP, Zheng H, Yue W, Conaway M, Santen RJ. Long-term exposure to tamoxifen induces hypersensitivity to estradiol. Clin Cancer Res 2004;10: 1530–4.
5. Nicholson RI, Hutcheson IR, Hiscox SE, et al. Growth factor signalling and resistance to selective oestrogen receptor modulators and pure anti-oestrogens: the use of anti-growth factor therapies to treat or delay endocrine resistance in breast cancer. Endocr Relat Cancer 2005;12 Suppl 1:29–36.
6. Osborne CK, Shou J, Massarweh S, Schiff R. Crosstalk between estrogen receptor and growth factor receptor pathways as a cause for endocrine therapy resistance in breast cancer. Clin Cancer Res 2005;11:865–70s.
7. Normanno N, Di Maio M, De Maio E, et al. Mechanisms of endocrine resistance and novel therapeutic strategies in breast cancer. Endocr Relat Cancer 2005;12:721–47.
8. Schiff R, Massarweh SA, Shou J, Bharwani L, Mohsin SK, Osborne CK. Cross-talk between estrogen receptor and growth factor pathways as a molecular target for overcoming endocrine resistance. Clin Cancer Res 2004; 10:331–6S.
9. Kim S, Ko H, Park JE, Jung S, Lee SK, Chun YJ. Design, synthesis, and discovery of novel *trans*-stilbene analogues as potent and selective human cytochrome P450 1B1 inhibitors. J Med Chem 2002;45:160–4.
10. Chun YJ, Kim S, Kim D, Lee SK, Guengerich FP. A new selective and potent inhibitor of human cytochrome P450 1B1 and its application to antimutagenesis. Cancer Res 2001;61:8164–70.
11. Chun YJ, Lee SK, Kim MY. Modulation of human cytochrome P450 1B1 expression by 2,4,3′,5′-tetramethoxystilbene. Drug Metab Dispos 2005;33:1771–6.
12. Yue W, Santen RJ, Wang JP, et al. Genotoxic metabolites of estradiol in breast: potential mechanism of estradiol induced carcinogenesis. J Steroid Biochem Mol Biol 2003;86:477–86.
13. Fan P, Wang J, Santen RJ, Yue W. Long term treatment with tamoxifen facilitates translocation of ERα out of the nucleus and enhances its interaction with epidermal growth factor receptor in MCF-7 breast cancer cells. Cancer Res 2007;67:1352–60.
14. Santen R, Jeng MH, Wang JP, et al. Adaptive hypersensitivity to estradiol: potential mechanism for secondary hormonal responses in breast cancer patients. J Steroid Biochem Mol Biol 2001;79:115–25.
15. Jeng MH, Yue W, Eischeid A, Wang JP, Santen RJ. Role of MAP kinase in the enhanced cell proliferation of long term estrogen deprived human breast cancer cells. Breast Cancer Res Treat 2000;62:167–75.
16. Wang S, Paris F, Sultan CS, et al. Recombinant cell ultrasensitive bioassay for measurement of estrogens in postmenopausal women. J Clin Endocrinol Metab 2005; 90:1407–13.
17. Jordan MA, Ojima I, Rosas F, et al. Effects of novel taxanes SB-T-1213 and IDN5109 on tubulin polymerization and mitosis. Chem Biol 2002;9:93–101.
18. Yao K, Lee ES, Bentrem DJ, et al. Antitumor action of physiological estradiol on tamoxifen-stimulated breast tumors grown in athymic mice. Clin Cancer Res 2000;6: 2028–36.
19. Shim WS, Conaway M, Masamura S, et al. Estradiol hypersensitivity and mitogen-activated protein kinase expression in long-term estrogen deprived human breast cancer cells *in vivo*. Endocrinology 2000;141: 396–405.
20. Gao N, Nester RA, Sarkar MA. 4-Hydroxy estradiol but not 2-hydroxy estradiol induces expression of hypoxia-inducible factor 1α and vascular endothelial growth factor A through phosphatidylinositol 3-kinase/Akt/FRAP pathway in OVCAR-3 and A2780–70 human ovarian carcinoma cells. Toxicol Appl Pharmacol 2004; 196:124–35.
21. Belleri M, Ribatti D, Nicoli S, et al. Antiangiogenic and vascular-targeting activity of the microtubule-destabilizing *trans*-resveratrol derivative 3,5,4′-trimethoxystilbene. Mol Pharmacol 2005;67:1451–9.
22. Jordan MA. Mitotic block induced in HeLa cells by low concentrations of paclitaxel (Taxol) results in abnormal mitotic exit and apoptotic cell death. Cancer Res 1996;56:816–25.
23. Jordan MA, Thrower D, Wilson L. Mechanism of inhibition of cell proliferation by *Vinca* alkaloids. Cancer Res 1991;51:2212–22.
24. Blajeski AL, Phan VA, Kottke TJ, Kaufmann SH. G_1 and G_2 cell-cycle arrest following microtubule depolymerization in human breast cancer cells. J Clin Invest 2002;110:91–9.
25. Sunters A, Madureira PA, Pomeranz KM, et al. Paclitaxel-induced nuclear translocation of FOXO3a in breast cancer cells is mediated by c-Jun NH_2-terminal kinase and Akt. Cancer Res 2006;66:212–20.
26. Wang TH, Wang HS, Soong YK. Paclitaxel-induced cell death: where the cell cycle and apoptosis come together. Cancer 2000;88:2619–28.
27. Gogvadze V, Orrenius S, Zhivotovsky B. Multiple pathways of cytochrome *c* release from mitochondria in apoptosis. Biochim Biophys Acta 2006;1757: 639–47.
28. Soldani C, Scovassi AI. Poly(ADP-ribose) polymerase-1 cleavage during apoptosis: an update. Apoptosis 2002; 7:321–8.
29. Jordan MA, Wilson L. Microtubules as a target for anticancer drugs. Nat Rev Cancer 2004;4:253–65.
30. Salmon ED, McKeel M, Hays T. Rapid rate of tubulin dissociation from microtubules in the mitotic spindle

in vivo measured by blocking polymerization with colchicine. J Cell Biol 1984;99:1066–75.
31. Nagata K, Puls A, Futter C, et al. The MAP kinase kinase kinase MLK2 co-localizes with activated JNK along microtubules and associates with kinesin superfamily motor KIF3. EMBO J 1998;17:149–58.
32. McLean GW, Carragher NO, Avizienyte E, Evans J, Brunton VG, Frame MC. The role of focal-adhesion kinase in cancer—a new therapeutic opportunity. Nat Rev Cancer 2005;5:505–15.
33. Shaw RJ, Cantley LC. Ras, PI(3)K and mTOR signalling controls tumour cell growth. Nature 2006; 441:424–30.
34. Landsverk KS, Lyng H, Stokke T. The response of malignant B lymphocytes to ionizing radiation: cell cycle arrest, apoptosis and protection against the cytotoxic effects of the mitotic inhibitor nocodazole. Radiat Res 2004;162:405–15.
35. Sunters A, Madureira PA, Pomeranz KM, et al. Paclitaxel-induced nuclear translocation of FOXO3a in breast cancer cells is mediated by c-Jun NH_2-terminal kinase and Akt. Cancer Res 2001;66:212–20.
36. Liu B, Fang M, Lu Y, Lu Y, Mills GB, Fan Z. Involvement of JNK-mediated pathway in EGF-mediated protection against paclitaxel-induced apoptosis in SiHa human cervical cancer cells. Br J Cancer 2001;85: 303–11.
37. Mansilla S, Priebe W, Portugal J. Mitotic catastrophe results in cell death by caspase-dependent and caspase-independent mechanisms. Cell Cycle 2006;5:53–60.

Effects of Tetramethoxystilbene on Hormone-Resistant Breast Cancer Cells: Biological and Biochemical Mechanisms of Action

Hoyong Park, Sarah E. Aiyar, Ping Fan, et al.

Cancer Res 2007;67:5717-5726.